

Spatio-temporal Receptivity of Boundary-Layers by Bromwich Contour Integral Method

T. K. Sengupta and A. Kameswara Rao

High Performance Computing Laboratory
Department of Aerospace Engineering
Indian Institute of Technology Kanpur
KANPUR 208 016, India
tksen@iitk.ac.in

1. Introduction

Transition from laminar to turbulent flow occurs via inherent instability of the former caused by the omnipresent background disturbances. While the motivation behind the famous experiments of [5] was to relate the instability with the disturbance level, most theoretical analyses, studies transition as an eigenvalue problem- in either temporal or spatial framework. Significant progress made by this approach is recorded in [2], while many issues still remain unresolved. For example, plane Couette and Poiseuille flow are found stable by eigenvalue analysis for certain parameter combinations, while lab experiments reveal them to be unstable. Classical approaches in this field, involve identifying equilibrium states whose stability is studied by eigenvalue analysis, by linearizing the governing mass and momentum conservation equation and then expressing it in the spectral plane after making the parallel flow assumption, leading to the well-known Orr-Sommerfeld equation. The least stable mode, often display wave-like nature and is said to produce the Tollmien-Schlichting (TS) waves.

In general fluid dynamic systems, it is not known *a priori* whether disturbances grow in space or in time or as spatio-temporal structures and this issue has not been resolved by instability studies. The alternative is to use receptivity studies where the response of the system is obtained with respect to impressed disturbances. For localized harmonic excitation, in [3] and [6] the assumption, that the response is at the frequency of the imposed excitation was made for the ease of the receptivity calculation and this is known as the *signal problem*. In [7] this assumption was removed and the complete spatio-temporal analysis was made using Bromwich contour integral method. For a zero pressure gradient boundary-layer, it was shown that this and the *signal problem* produces identical response field, for those cases where the system is spatially unstable. In a recent study [8], it has been shown that these two approaches do not produce identical results for spatially stable systems and indicates the necessity of performing spatio-temporal receptivity studies by the Bromwich contour integral method.

In the present study, we show the composite nature of the response field obtained by the Bromwich contour integral method. We identify the near- and far-field response of a stable system for the zero pressure gradient boundary layer, and finally explain the structure of the near-field analytically.

2. Problem Formulation

We have investigated the response of a zero pressure gradient boundary layer excited by a harmonic source at the wall, at a circular frequency β_0 , as shown in Figure 1. We represent the disturbance stream function by,

$$\psi(x, y, t) = \int \int_{Br} \phi(\alpha, \beta, y) e^{i(\alpha x - \beta t)} d\alpha d\beta \quad (1)$$

where Br indicate the Bromwich contours followed in evaluating the above integral in the complex α and β plane - β_0 appearing via the wall boundary condition [8]. The mathematical basis of Bromwich contour integral is given in [4, 9] and its application for the present problem can be seen from [7, 8].

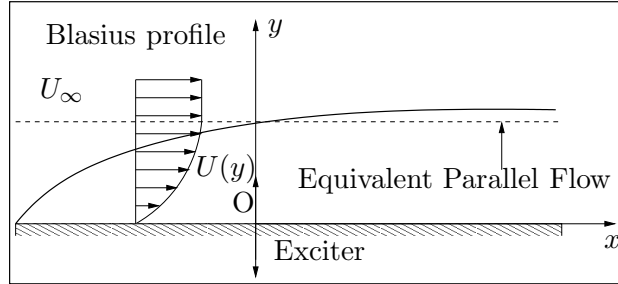


Figure 1: Harmonic excitation of a parallel boundary layer corresponding to the location of the exciter.

The posed problem is solved by linearizing the Navier-Stokes equation in the spectral planes and expressing it as the Orr-Sommerfeld equation given by,

$$(U - \beta/\alpha)(\phi'' - \alpha^2 \phi) - U''\phi = \frac{1}{i\alpha Re}(\phi^{iv} - 2\alpha^2 \phi'' + \alpha^4 \phi) \quad (2)$$

where $U(y)$ is the mean flow and the Reynolds number is based on displacement thickness. The choice of Bromwich contours in β - plane is restricted by causality principle and in the α - plane is made in such a way that all the eigenvalues corresponding to the downstream propagating modes remain above it. If cartesian disturbance velocity components are denoted by u and v , respectively, then the boundary conditions for solving Equation (2) at $y = 0$ are: $u = 0$, $\psi(x, 0, t) = H(t)\delta(x)e^{-i\beta_0 t}$ and for $y \rightarrow \infty$: $u, v \rightarrow 0$ where $H(t)$ is the Heaviside function and $\delta(x)$ represents the Dirac delta excitation at the origin of the frame. To discuss the spatio-temporal growth of waves for Blasius boundary layer, two spatially stable cases are considered marked as B and D in Figure 2, that represents the neutral curve in $(Re - \beta_0)$ plane.

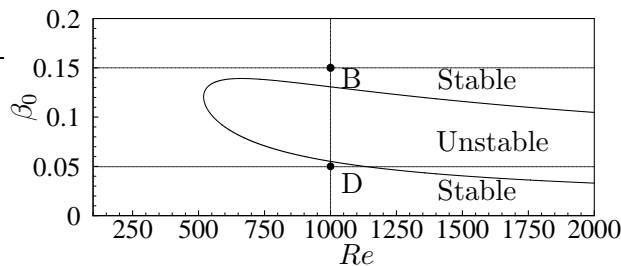


Figure 2: Neutral curve for the Blasius boundary layer.

3. Disturbance flow-field

Here, a Blasius boundary layer is considered whose spatial normal modes are evaluated by grid-search technique employing compound matrix method [7] for $Re = 1000$ and $\beta_0 = 0.05$ and 0.15 and their wave properties are given in Table-1. For these parameters, existing spatial modes are

Table 1: The wave properties for the points B & D identified in Fig. 2

β_0	α_r	α_i
0.05 (D)	1) 0.0621 413	0.0696 594
	2) 0.1607 670	0.0015 206
0.15 (B)	3) 0.1894 256	0.3226 357
	4) 0.2728 701	0.1675 585
	5) 0.3940 036	0.0104 936

all damped- one set corresponding to $\beta_0 = 0.05$ (identified as 1 and 2) are below the neutral curve and the other set corresponding to $\beta_0 = 0.15$ (identified as 3-5 in Table 1).

Equation (2) is solved along the Bromwich contours: (i) $-20 \leq \alpha_r \leq 20$; $\alpha_i = -0.001$ and (ii) $-1 \leq \beta_r \leq 1$; $\beta_i = 0.02$ - such that the causality principle is not violated and waves travel in the correct direction. Obtained ϕ 's are used to reconstruct the disturbance field in Equation (1) and the velocity field are as plotted in Figure 3 for the case of *B* at the indicated time instants. While Table 1 shows all three spatial modes as stable, the contour integral results in Figure 3 show (i) the near-field given by the local solution and the far-field that consists of (ii) a decaying wave and (iii) a temporally growing wave-packet.

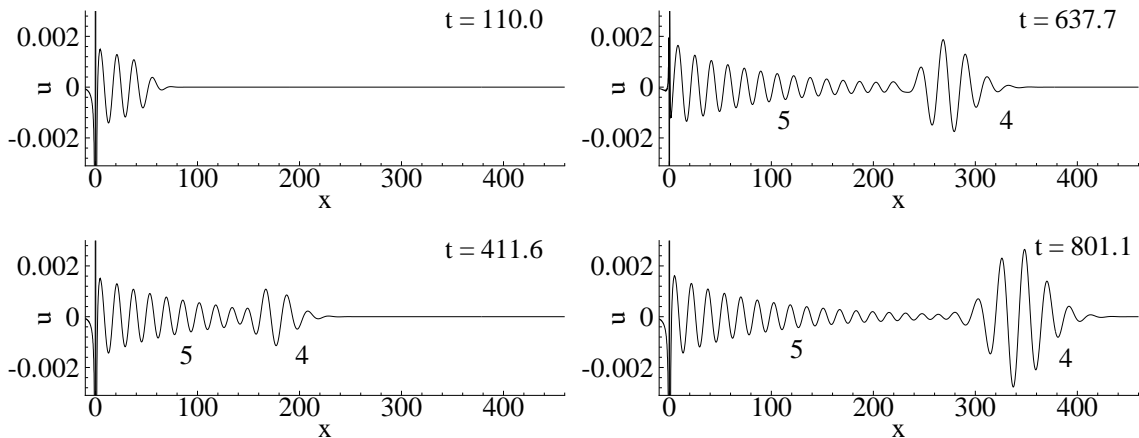


Figure 3: Streamwise disturbance velocity plotted as a function of x at different t for $\beta_0 = 0.15$, $Re = 1000$ at $y = 0.278$

After long time, the decaying wave corresponds to Mode 5 and the growing wave-front corresponds to Mode 4 of Table 1. Effect of Mode 3 is not visible due to its extremely large decay rate. In Figure 4, Fourier-Laplace transform of the signal is shown for $t = 801.1$, that identifies Modes 4 and 5. In this figure, the dashed lines indicate the location of the three modes for this case.

In Figure 5, u is shown plotted against x at the indicated time instants for the case of point D of Figure 2. This also shows a similar disturbance with near- and far-field structures. In Figure 6, the corresponding Fourier-Laplace transform of the signal at $t = 788$ is shown. In this case, the asymptotic decaying signal correspond to Mode 2, while the effect of Mode 1 is not visible here. The growing wave-front corresponds to the packet to the right of Mode 2. In Figures 3 and 5, one notices the near-field to represent a sharp change of the variable- although there is upstream penetration of the disturbance field with respect to the exciter. This aspect of the near-field is discussed next.

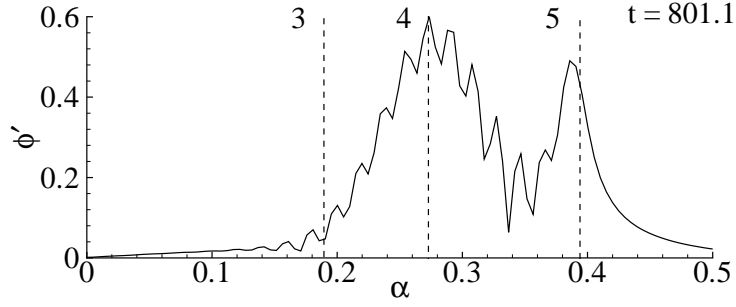


Figure 4: FFT of streamwise disturbance velocity plotted as a function of α for point B.

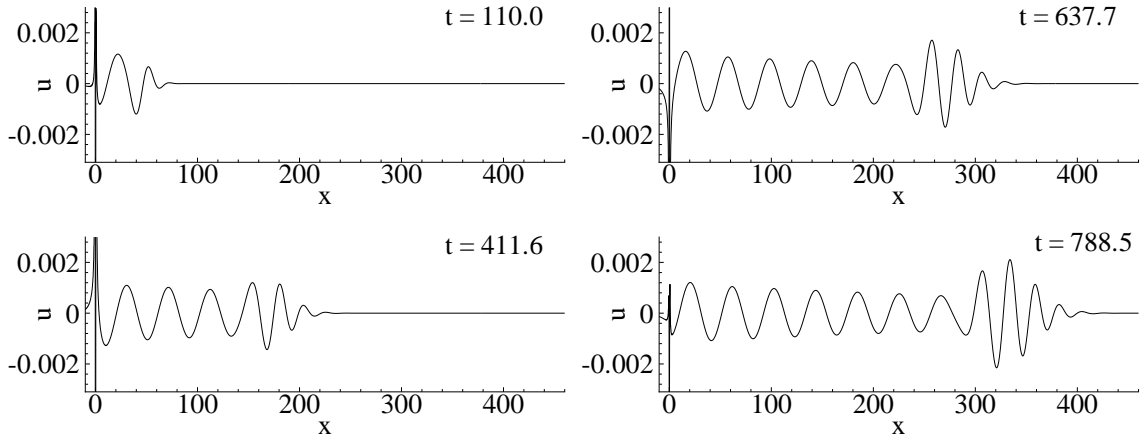


Figure 5: Streamwise disturbance velocity plotted as a function of x at different t for $\beta_0 = 0.05$, $Re = 1000$ at $y = 0.278$

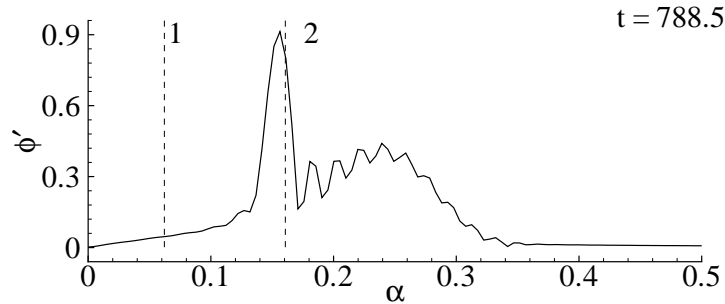


Figure 6: FFT of streamwise disturbance velocity plotted as a function of α for point D.

4. Near-field Response by Localized Excitation

We have noted in [7, 8] that there are no differences in the response between the spatial and spatio-temporal analysis for unstable wave cases. Thus, to understand the near-field structure we consider the unstable case with $Re = 1000$ and $\beta_0 = 0.1$ so that the resulting analysis is easier and tractable. In Figure 7, the resultant response field for this case is shown only in the near vicinity of the exciter in three frames with time interval marked in one complete cycle of its excursion.

From the displayed frames, it is noted that this component is not a traveling disturbance- it simply pulsates at the location of the exciter. A simple calculation reveals that this pulsation is at the excitation frequency, $\beta_0 = 0.1$. The top frame shows the variation of local solution as

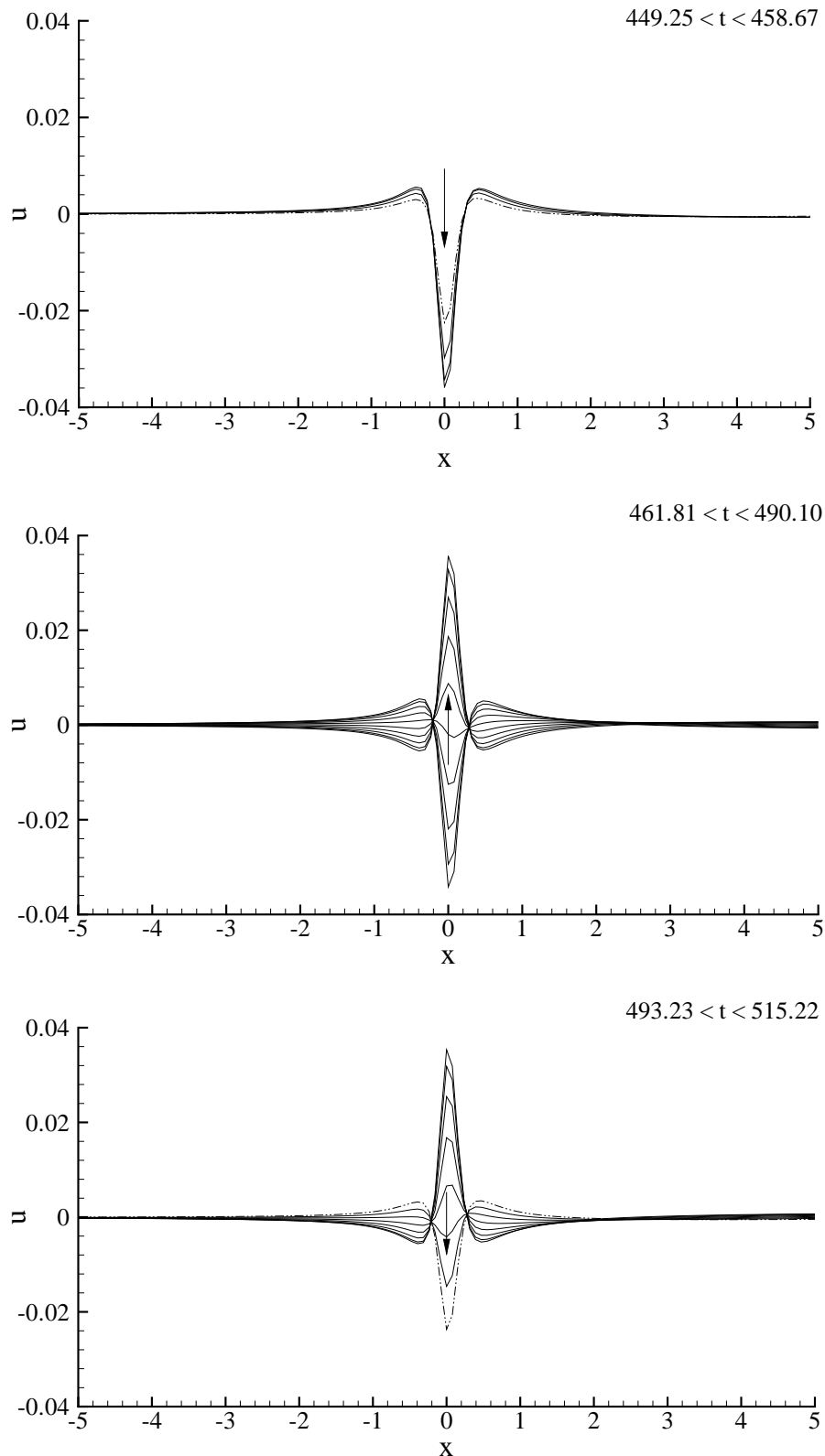


Figure 7: Local solution for u as a function of x for $\beta_0 = 0.1$ and $Re = 1000$ at $y = 0.278$

it decreases in the time range shown. In the middle frame, the excursion is shown as the local solution increases with time and the bottom frame shows variation from the highest value to the starting location. In the following we attempt to explain the feature of the local solution.

For the *signal problem* considered in this section, the disturbance stream function is given by,

$$\psi_c(x, y, t) = \int_{Br} \phi(\alpha, \beta_0, y) e^{i(\alpha x - \beta_0 t)} d\alpha \quad (3)$$

and the Laplace transform is governed by Equation (2), with β replaced by β_0 . The Bromwich contour is fixed in the α - plane only. In the context of exploring relationship between the original (ψ_c) and the image (ϕ), two theorems due to Abel and Tauber are relevant (as given in [9]). If one is interested in the behaviour of ψ_c , far away from the exciter ($x \rightarrow \infty$), then it is located by ϕ in the neighbourhood of the origin in the α - plane (Abel's theorem). This implies that the far-field solution is determined by the singularities of ϕ (the poles and branch points) near the origin, in the α - plane. In contrast, ψ_c in the near vicinity of the exciter is decided by ϕ at $\alpha \rightarrow \infty$ (Tauber theorem).

Thus, for the near-field solution, one needs to find the contribution of ϕ in Equation (3) by the Bromwich contour segment when $\alpha \rightarrow \infty$. In Figure 8, we have shown a rudimentary integration contour that can be used to perform the integral of (3) in the α - plane. The semi-circular arc $C \equiv C_1 \cup C_2 \cup C_3$, in the limit $\rho \rightarrow \infty$ represents half of the contour that actually represents the point at infinity, in the α - plane.

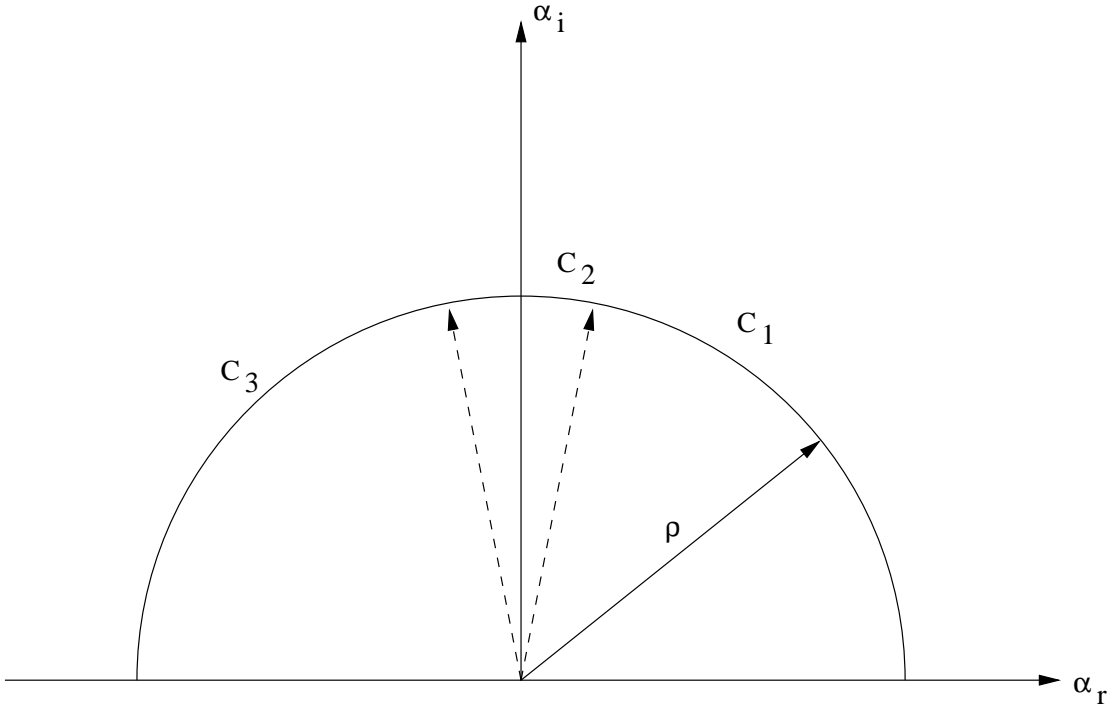


Figure 8: Integration contour in α -plane for the essential singular point.

One notes here that in many indefinite integrals of the type given by Equation (3), one actually uses Jordan's lemma and ignores the contribution coming from this semi-circular arc. In (3), ψ_c contribution from the semi-circular arc would vanish if and only if the denominator of the integrand is at least two units higher than the degree of the numerator (see [1]) i.e. if and only if

$$|\phi(y, \alpha, \beta_0)| < \frac{k}{|\alpha^2|} \quad (4)$$

for $\alpha \rightarrow \infty$. Thus, it remains to be shown if the Jordan's lemma is valid for the present case. To investigate this, we analytically obtain $\phi(y, \alpha)$ as a function of $\epsilon_1 (= \frac{1}{\alpha})$ by a singular

perturbation analysis for $\alpha \rightarrow \infty$. With this small parameter ϵ_1 , on the semi-circular arc of Figure 8 one can define $\alpha = \rho\theta$, where ρ is the radius of the arc and $\theta = \theta_r + i\theta_i$ is the complex phase of α . To determine ϕ for $\alpha \rightarrow \infty$, one can perform the singular perturbation analysis and obtain the inner solution ϕ_i , by reducing Equation (2) to

$$\phi_i^{iv} - 2\theta^2\phi_i'' + \theta^4\phi_i = 0 \quad (5)$$

where the derivatives are with respect to the independent variable $Y = \frac{y}{\epsilon_1}$. It is noted that the governing equation along C , reduces to $\nabla^4\psi = 0$, that is independent of β_0 and Re . The solution of Equation (5) is obtained in the original co-ordinates as,

$$\phi(y, \alpha) = (1 + \alpha y)e^{-\alpha y} \quad \text{for } \alpha_r > 0(\text{on } C_1) \quad (6)$$

$$\phi(y, \alpha) = (1 - \alpha y)e^{\alpha y} \quad \text{for } \alpha_r < 0(\text{on } C_3) \quad (7)$$

One can similarly obtain the expression for ϕ along C_2 of the semi-circular contour. These analytical solutions clearly reveal that for this problem one cannot use the Jordan's lemma, as the conditions of Equation (4) is not satisfied. It would therefore be interesting to use Tauber's theorem to find out the contribution to ψ_c in Equation (4), by the analytical solutions in (6)-(7). Use of these in (4), yield the following solution,

$$\begin{aligned} \psi_c(x, y, \rho, t) = & [\cos(\rho y)e^{-\rho x} + \frac{ie^{i\rho z}}{z}(1 + \rho y + \frac{iy}{z}) - \frac{ie^{-i\rho\bar{z}}}{\bar{z}}(1 + \rho y - \frac{iy}{\bar{z}}) \\ & - \frac{ie^{-\rho z + iz}}{z}(1 + \frac{iy}{z} + y + i\rho y) + \frac{ie^{-\rho\bar{z} - i\bar{z}}}{\bar{z}}(1 - \frac{iy}{\bar{z}} - i\rho y + y)] \frac{e^{-i\beta_0 t}}{2\pi} \end{aligned}$$

where $z = x + iy$ and $\bar{z} = x - iy$. For the limit $\rho \rightarrow \infty$, this solution when plotted would not reveal physical solution, as the plots indicate very high frequency oscillations. However, a very interesting result emerges when we inspect this solution at $y = 0$ that simplifies to,

$$\psi_c(x, 0, \rho, t) = [e^{-\rho x} \{1 + \frac{2\sin\rho x}{x}\} + \frac{2\sin\rho x}{x}] \frac{e^{-i\beta_0 t}}{2\pi}$$

In the limit $\rho \rightarrow \infty$, the first term does not contribute, while the second term is the Dirichlet function [9]- an approximation for the Dirac Delta function. Thus, the quantity which is traditionally considered negligible by Jordan's lemma turns out to support the applied boundary condition.

This analysis explains the nature of the near-field of the solution obtained by the receptivity analysis. An inspection of Figures 3 and 5 reveal that the near-field of the solution are identical, even when β_0 value changes three-fold. It can also easily be shown that the near-field is independent of Re - as shown in the above analysis.

References

- [1] G. Arfken, *Mathematical Methods for Physicists*, (3rd Edn.) (Acad. Press, Orlando, Florida, USA) (1985).
- [2] P.G. Drazin and W.H. Reid, *Hydrodynamic Stability*, (Cambridge Univ. Press, Cambridge, U.K.) (1981).
- [3] M. Gaster, "On the generation of spatially growing waves in a boundary layer", *J. Fluid Mech.*, **22**, 433-441 (1965).
- [4] A. Papoulis, *The Fourier Integral and Its Application*, (McGraw Hill, New York, USA) (1962).

- [5] O. Reynolds, *Scientific Papers*, (Cambridge Univ. Press, Cambridge, U.K.) (1901).
- [6] T.K. Sengupta, "Impulse response of laminar boundary layer and receptivity", Proc. of 7th *Int. Conf. Num. Meth. Laminar & Turbulent Flows*, **7**(1), 45-53 (Pineridge Press, Swansea, U.K.) (1991).
- [7] T.K. Sengupta, M. Ballav and S. Nijhawan, "Generation of Tollmien-Schlichting waves by harmonic excitation", *Physics of Fluids*, **6**(3), 1213-1222 (1994).
- [8] T.K. Sengupta, A.Kameswara Rao and K. Venkatsubbaiah, "Spatio-temporal growing wavefronts in spatially stable boundary layers", *Physical Review Letters*, **96**, 224504 (2006).
- [9] B. Van der Pol and H. Bremmer, *Operational Calculus Based on Two-Sided Laplace Integral*, (Cambridge Univ. Press, Cambridge, U.K.) (1959).